Computers chem. Engng, Vol. 14, No. 4/5, pp. 401–413, 1990
Printed in Great Britain.

0098-1354/90 $3.00 + 0.00

MU-OPTIMAL *LV*-CONTROL OF DISTILLATION COLUMNS

S. SKOGESTAD and P. LUNDSTRÖM
Chemical Engineering, Norwegian Institute of Technology (NTH), N-7034 Trondheim, Norway

(*Received* 18 *October* 1989; *received for publication* 29 *November* 1989)

Abstract—Two-point composition control using the *LV*-configuration is examined. In spite of high steady-state RGA-values it is shown for seven example columns that the *LV*-configuration may yield acceptable robust performance using single-loop controllers provided measurement delays are not too large.

In order to investigate the level of modelling detail that is required for effective control, five process models of different complexity are studied. It is demonstrated that flow dynamics should be included in a column model which is to be used for controller design.

The structured singular value (Mu or μ) is used as a robust performance index. To use this index one must define performance using the H_∞ framework. The issue of selection of performance and uncertainty weights is critical in this procedure, and is discussed in detail in the paper.

1. INTRODUCTION

Distillation is one of the most common unit operations in the chemical industry, and is probably the most extensively studied from a control point of view. Still, most distillation columns in industry are not operated under automatic feedback control of both top- and bottom-composition (two-point control) which would be optimal from an economic point of view. Rather, control of only one composition (one-point control) is used on most industrial columns. In this paper we will examine if it is possible to achieve good control of both compositions using the *LV*-configuration. Secondly, since the structured singular value is used as a performance index, we shall attempt to give some guidelines on how to formulate a meaningful problem statement within this framework.

The *LV*-configuration involves using reflux L and boilup V for composition control with the top and bottom levels controlled by distillate D and bottoms B (Fig. 1). This configuration is commonly used in industry for one-point composition control. However, it is well-known that severe interactions often make two-point control difficult with this configuration. The interactions are caused by the fact that L and V affect both compositions in a similar manner. One measure often used to quantify the interactions is the relative gain array (RGA), (Bristol, 1966). The steady-state RGA-elements are often very high for the *LV*-configuration indicating severe problems with interactions. However, the RGA-elements are much lower at high frequency, indicating that control may not be that difficult after all.

Some questions we would like to answer with respect to two-point composition control using the *LV*-configuration are the following:

1. Is it possible to achieve good control behavior (good performance) with the *LV*-configuration when model uncertainty and possible changes in the operating point are included?
2. Is it possible to avoid the severe interactions with a proper design of the controller?
3. How much achievable performance is lost by insisting on using single-loop PI- or PID-controllers?
4. What factors in the model are important to include in order to design a controller which retains its performance when applied to the real column?
   (i) the steady-state and dominating dynamics (τ_1);
   (ii) the dynamics of the internal flows (τ_2);
   (iii) the high-frequency flow dynamics (θ_L);
   (iv) other high-frequency dynamics such as measurement delays?
5. Is there a correlation between large steady-state RGA-values and achievable robust performance when single-loop controllers are used?
6. Do the same controller tunings work satisfactorily both for two-point and one-point control?
7. Is it possible to find any simplified tuning rules for the SISO PID-controller case?

We will attempt to answer most of these questions in this paper. Some of the issues mentioned above, for example the effect of model uncertainty and changes in operating point, have been addressed previously by Skogestad *et al.* (1988) and Skogestad and Morari (1988a). This paper is partly a continuation of the latter work, but here models which also include flow dynamics will be used. Arkun and Morgan (1988) considered the effect of various sources of model uncertainty for distillation columns and concluded

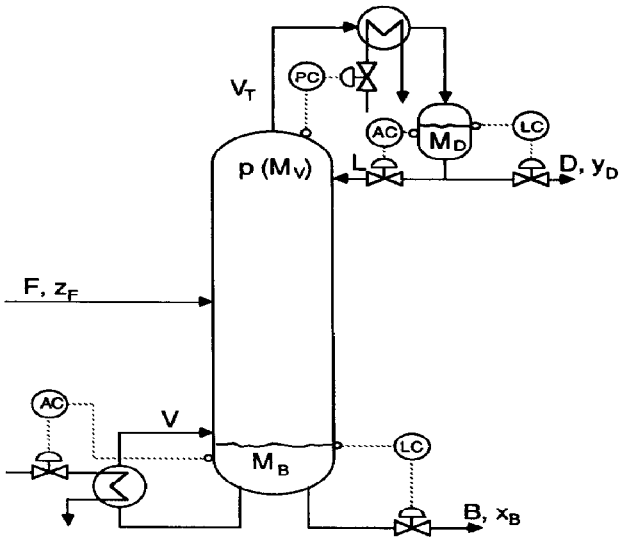

Fig. 1. Single-loop two-point control using the LV-configuration.

that use of the structured singular value reduces the conservativeness compared to using singular values. McDonald *et al.* (1988) represented nonlinearity caused by changes in operating point as model uncertainty. However, as pointed out by Skogestad and Morari (1988a) this approach is not rigorous and may easily be very conservative, as is also clear from the results of McDonald *et al.* In this paper we will therefore consider only one operating point for each column, and the uncertainties represent "true" uncertainty or neglected dynamics (and not nonlinearity). The effect of changes in operating point may be counteracted by using logarithmic compositions (Skogestad and Morari, 1988a, b).

In this paper we design and analyze controllers by computing the structured singular value μ introduced by Doyle (1982), which is a measure of robust performance. This means that the best controller is the one that gives the best worst-case response. By worse-case we mean the worst combination of possible disturbances, setpoint changes and model errors. The main advantage with μ is that it provides a rigorous and simple way of comparing the robust performance of different controllers without having to perform a large number of simulations. We will not discuss the theory of robust control in this paper, and readers not familiar with μ-analysis are recommended to consult the paper of Skogestad *et al.* (1988). However, we shall try to give some insight into the practical use of the method, in particular, on how to choose reasonable performance and uncertainty weights.

An important reason for using robust performance as a measure for comparison is that the control behavior of the LV-configuration may be very sensitive to model error. This was shown by Skogestad and Morari (1988a) for two example columns (A and C). They found that although an inverse-based controller (using a dynamic decoupler) gave excellent nominal response (perfect decoupling and very fast response), the response with 20% uncertainty on the manipulated inputs gave extremely poor response. This result has been known qualitatively for a long time, but one advantage with the μ-analysis is that it confirmed this result in a rigorous manner. One lesson to learn was therefore that model uncertainty should be included in the problem definition in order to penalize this kind of inverse-based controllers.

Another result of the paper by Skogestad and Morari (1988a) was that simple PI-controllers seemed to perform quite well, but it was claimed in that paper that they were somewhat more sluggish than the μ-optimal controller. Actually, it turns out that the PI-controller used by Skogestad and Morari (1988a) was not very well tuned, and the results presented in the present paper demonstrate that simple PI- or PID-controllers may be tuned to give robust performance (that is, $\mu_{RP} < 1$) and that these controllers seem to be close to the best achievable using a full linear multivariable controller.

The RGA has traditionally been evaluated at steady-state only, but more recently the usefulness of the RGA as a function of frequency has become clear. For example, Skogestad and Morari (1987) argue that large values in the RGA at frequencies close to the system's closed-loop bandwidth indicate a plant that is fundamentally difficult to control (with any linear controller). Nett (1987) argues that for single-loop control the diagonal elements of the RGA should be close to one at frequencies corresponding to the closed-loop bandwidth. The usefulness of the frequency-dependent RGA as a measure of expected control quality is demonstrated in this paper.

2. PROBLEM DEFINITION

2.1. Uncertainty

To evaluate robust performance with the structured singular value we have to define performance and uncertainty. One source of uncertainty which always occurs in practice, and which generally limits achievable closed-loop performance (e.g. Skogestad *et al.*, 1988) is input uncertainty. This is the only source of uncertainty included in this paper. At steady-state the input error may typically be about 20%, but it increases at higher frequency and eventually exceeds 100% because of uncertain or neglected high-frequency dynamics, such as valve dynamics or time delays. Let ϵ denote the allowed steady-state relative error on each input. In addition, let θ be the allowed time delay error (may also represent neglected dynamics corresponding in phase lag to a time delay of θ). If a time delay $e^{-\theta s}$ is neglected, that is, modelled as 1, then a close upper bound on the magnitude of the relative error $(e^{-\theta s} - 1)/1$ is given by $\theta s/(1 + \theta s/2)$ (using a

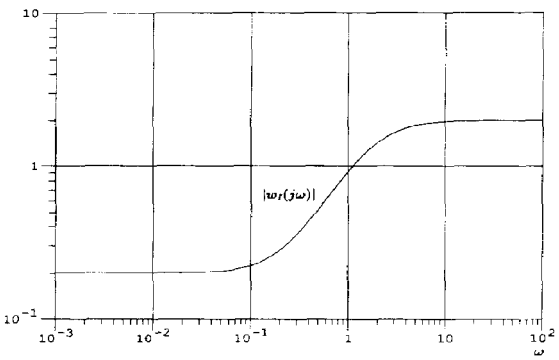

Fig. 2. Uncertainty weight $|w_I(j\omega)|$ [equation (1)] with $\epsilon = 0.2$ and $\theta = 1$ min.

first-order Padé approximation). Adding this with the constant term ϵ and assuming $\epsilon \ll 2$ yields the following weight for the overall multiplicative (relative) input uncertainty:

$$w_I(s) = \epsilon \frac{\frac{\theta}{\epsilon}s + 1}{\frac{\theta}{2}s + 1}. \quad (1)$$

We use the same weight as Skogestad and Morari (1988a) and choose $\epsilon = 0.2$ (20%) and $\theta = 1$ min. The weight is shown graphically as a function of frequency in Fig. 2.

We would like to stress that an input uncertainty of 20% by no means is large in a practical situation. It is often argued that input uncertainty may be reduced by measuring the flows accurately. This is correct, but only to a limited extent: (1) reliable measurements of flow during changing conditions in industrial operation is difficult; (2) the uncertainty is on the *change* in the flow and not on its absolute value. This means that we might have 20% input error even if the absolute error is much smaller. As an example, assume we want to increase L from 100 to 110. However, because of 1% measurement error the actual change is from 101 to 109, that is, the actual change is eight instead of the believed 10, corresponding to a gain error of 20%.

2.2. Performance

Performance is defined in terms of the H_∞-norm of some transfer function. This may be viewed as a direct generalization of the frequency domain performance specifications used in classical control for single-input–single-output (SISO) systems. Since this norm is not well-known for most readers, some discussion on its significance and also on the selection of reasonable performance weights is included.

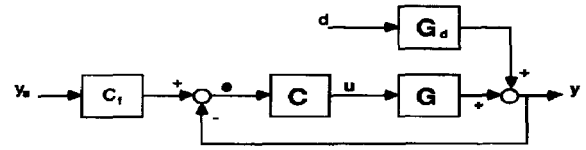

Fig. 3. Block diagram of conventional feedback system.

2.2.1. General H_∞-norm. A block diagram of a conventional feedback system with disturbances d and setpoints y_s is shown in Fig. 3. The most general way to define performance in the H_∞-framework is to consider the H_∞-norm of the closed-loop transfer function E between external normalized inputs $\hat{d}_I$ (disturbances, noise, setpoints) and normalized errors (outputs) $\hat{e}_O$ (may include $y - y_s$, manipulated inputs u which should be kept small, etc.). The weights are usually chosen such that magnitude (in terms of the two-norm) of the normalized external inputs are less than one at all frequencies, i.e. $\max_\omega \|\hat{d}_I(j\omega)\|_2 \equiv \|d_I\|_\infty \leq 1$, and such that for acceptable performance the normalized errors are less than one at all frequencies, i.e. $\|\hat{e}_O\|_\infty < 1$. With $\hat{e}_O = E\hat{d}_I$ this is equivalent to requiring:

$$\max_\omega \bar{\sigma}[E(j\omega)] \equiv \|E\|_\infty < 1. \quad (2)$$

Use of the maximum singular singular value $\bar{\sigma}$ (E) guarantees that the worst-case *direction* of E satisfies the performance criteria. For the system in Fig. 3 we would have to define weights W_d, W_s, W_e and W_u in order to normalize the signals to magnitude 1 and the transfer function E would be given as shown by the dotted box in Fig. 4. W_e might be a diagonal matrix of constants specifying how well a specific output should be controlled. W_u may be close to a pure differentiator (s) if we want to penalize fast changes in the inputs. Note that it is only the magnitude of the weights that matters; they should therefore be stable and minimum phase.

2.2.2. Bounds on the sensitivity function. The approach above is general and may be needed in some cases, for example, if it is important to penalize one

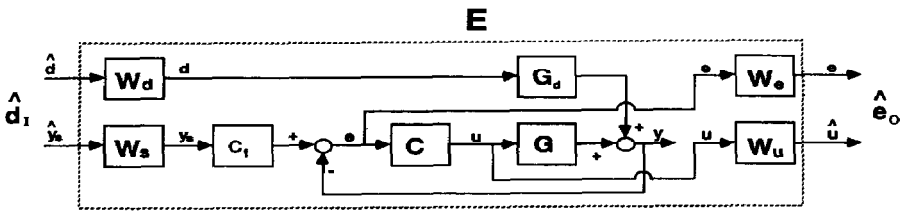

Fig. 4. Example of transfer function E used for general H_∞-performance.

or more of the input signals directly (though use of input uncertainty will penalize large inputs indirectly). However, in many cases it is simpler and more instructive to translate the desired performance specifications into an upper bound $1/|w_P|$ on the frequency plot of the magnitude of the sensitivity function S:

$$\bar{\sigma}(S(j\omega)) < 1/|w_P(j\omega)|, \forall\omega, \quad (3)$$

where

$$S(j\omega) = [I + G(j\omega)C(j\omega)]^{-1}. \quad (4)$$

This performance specification may *equivalently* be formulated as a bound on the H_∞-norm of the weighted sensitivity function $w_P S$:

$$\max_\omega \bar{\sigma}[w_P S(j\omega)] \equiv \|w_P S\|_\infty < 1. \quad (5)$$

The concept of bandwidth, which is here defined as the frequency where $\bar{\sigma}(S)$ (or possibly its low-frequency asymptote) first crosses one, is closely related to this performance specification. In addition, most classical frequency domain specifications may be captured by this approach.

Classical frequency domain specifications—For example assume that the following specifications are given in the frequency domain:

1. Steady-state offset less than A.
2. Closed-loop bandwidth higher than ω_B.
3. Amplification of high-frequency noise less than a factor M.

These specifications may be reformulated in terms of equation (3) using:

$$w_P(s) = \frac{1}{M}\frac{\tau_P s + 1}{\tau_P s + A/M}, \quad \text{with } \tau_P = 1/M\omega_B \quad (6)$$

and the resulting bound $1/|w_P(jw)|$ is shown graphically in Fig. 5.

General case—In the multivariable case the generalized weighted sensitivity is $W_{P1} S W_{P2}$. For example, one may use different bounds on the sensitivity function for various outputs. Assume we want the response in channel 1 to be about 10 times faster than

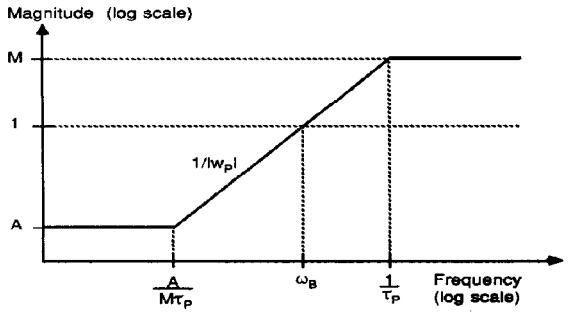

Fig. 5. Asymptotic plot of $1/w_P = M(\tau_P s + A/M)/(\tau_P s + 1)$ where $\tau_P = 1/M\omega_B$ [equation (6)] $|S(j\omega)|$ should lie below $1/|w_P|$ to satisfy classical frequency-domain specifications in terms of A, M and ω_B.

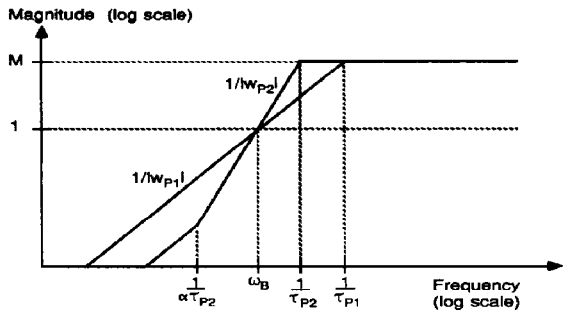

Fig. 6. Asymptotic plots of $1/w_{P1} = M\tau_{P1}s/(\tau_{P1}s + 1)$ and $1/w_{P2} = M\tau_{P2}s(\tau_{P2}s + 1/\alpha)/(\tau_{P2}s + 1)^2$.

that in channel 2. Then we might use the performance specification:

$$\|W_P S\|_\infty < 1; \quad W_P = \begin{pmatrix} w_{P11} & 0 \\ 0 & w_{P22} \end{pmatrix}, \quad (7)$$

with $\omega_{B11} = 10\omega_{B22}$. In this paper we shall use the same performance specifications for all channels, that is $W_P = w_P I$.

Specifications on disturbance rejection—To illustrate how specifications on disturbance rejection may be reformulated as bounds on the weighted sensitivity consider Fig. 4 and evaluate the transfer function from normalized disturbances to normalized errors:

$$\hat{e} = W_e S G_d W_d \hat{d}. \quad (8)$$

Consider the following special monovariable (SISO) case: (i) $W_e = 1$ (that is, the allowed error is the same at all frequencies and scaling has been applied to G and G_d such that an error $\hat{e}$ of magnitude 1 is the largest we can accept); (ii) disturbance model $G_d = k_d(1 + \tau_d s)$; (iii) disturbances at any frequencies are allowed, that is $W_d = 1$; and (iv) G_d has been scaled such that disturbances $\hat{d}$ are less than one in magnitude. The performance specification is then $\|W_e S G_d W_d\|_\infty = \|G_d S\|_\infty = \|w_P S\|_\infty < 1$. In addition to disturbance rejection we may require: (1) integral action, and (2) that the amplification of high-frequency disturbances (noise) is less than M, where $M > 1$. This may be done by increasing the performance weight ("tightening the specifications") at low and high frequencies by: (1) extending the slope of G_d at low frequencies such that w_P contains an integrator; and (2) setting $w_P = 1/M$ at high frequencies. The overall weight becomes:

$$w_{P1}(s) = \frac{1}{M}\frac{\tau_{P1}s + 1}{\tau_{P1}s}, \quad \text{with} \quad \tau_{P1} = \frac{\tau_d}{k_d M}. \quad (9)$$

This weight is identical to the weight obtained before from direct specifications on S [equation (6) with $A = 0$]. We see that $|S|$ at intermediate frequencies should increase with a slope of about one (on a log–log frequency plot). The frequency where the asymptote of the weight crosses one (bandwidth requirement) is $w_{B1} = 1/(M\tau_{P1}) = k_d/\tau_d$. In addition, we shall consider a weight w_{P2} where $|S|$ should

increase with a slope of about two at intermediate frequencies:

$$w_{P2}(s) = \frac{1}{M}\frac{(\tau_{P2}s + 1)^2}{\tau_{P2}s(\tau_{P2}s + 1/\alpha)}, \quad \text{with } \alpha > 1. \qquad (10)$$

Such a weight could have been derived by selecting $W_d = 1/s$ in the above procedure. It may be more appropriate for step disturbances which affect the outputs initially as ramps. The bandwidth requirement in this case is $w_{B2} = 1/(\sqrt{M}\tau_{P2})$.

In the *multivariable* case it is more appropriate to use matrix-valued weights, that is, the performance measure is $\|W_P S G_d\|_\infty$ where G_d is a vector expressing the effect of the disturbance d on the outputs. In this case $\bar{\sigma}[SG_d(j\omega)]$ may be significantly smaller than $\bar{\sigma}[S(j\omega)]\bar{\sigma}[G_d(j\omega)]$ when G_d is in the "good" direction corresponding to the large plant gains (see Skogestad *et al.*, 1988), and the bandwidth requirement imposed by disturbances is less than that given above. Furthermore, if the column elements in G_d are different in magnitude then the bandwidth requirements for each loop become different. However, for the example columns used in this paper, we decided to use a simple scalar weight (and use $\|w_P S\|_\infty$ as the performance measure) even though our distillation example is a multivariable problem.

Weights used in examples—For the distillation column example we shall use the performance weights w_{P1} and w_{P2} above with numerical values $M = 2$, $\alpha = 4$, $\tau_{P1} = 10$ min and $\tau_{P2} = 16.7$ min (unless other values for τ_P specified). This choice for τ_{P2} makes $|w_{P2}(j\omega)|$ almost identical to $|w_{P1}(j\omega)|$ at high frequencies, but different at low frequencies. This is shown in Fig. 7 where $1/|w_{P1}|$ and $1/|w_{P2}|$ are shown as functions of frequency. The first weight w_{P1} is identical to the one used by Skogestad *et al.* (1988) and Skogestad and Morari (1988a). Both weights require a controller with integral action, give a bandwidth requirement of about $\omega_B = 1/20\ \text{min}^{-1}$, and have a maximum allowed peak $M = 2$ for $|S|$. The second weight requires somewhat more preformance at low frequencies. However, the difference is not large since the value of α is rather small.

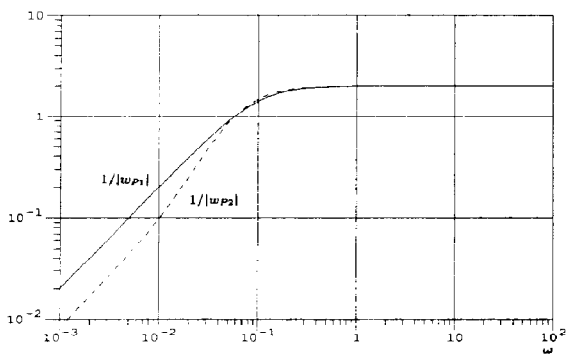

Fig. 7. Performance weights $1/w_{P1}(\tau_{P1} = 10\ \text{min})$ and $1/w_{P2}(\tau_{P2} = 16.7\ \text{min})$ used in examples.

2.2.3. Prefilter for setpoints, c_f. The requirements on how to best shape S for disturbance rejection are generally different from those for command (setpoint) following. To account for this one should take advantage of the fact that the setpoint y_s is known and use a prefilter c_f (two degrees of freedom controller, see Fig 3). In particular, there is generally no requirement for distillation columns to track fast setpoint changes in composition. In the simulations we therefore use a simple first-order filter:

$$c_f(s) = \frac{1}{5s + 1}, \qquad (11)$$

which means that we do not require the system to track setpoint changes with a time constant less than 5 min. This leads to more moderate initial control actions, for example, when there are step changes in y_s. Note the prefilter c_f is not used in the μ-analysis or in the controller design which is based on minimizing the H_∞-norm of $w_P S$.

2.3. Robust stability and performance

Robust stability (RS)—The system is said to be robustly stable if it is stable for all uncertainties defined by the uncertainty description. In this case it means that the system should be stable for all the possible input errors defined above. Mathematically, this may be tested by computing at each frequency μ of the matrix $N_{RS} = w_I CSG$ with respect to the structure of the uncertainties (a diagonal 2×2 matrix) (Skogestad and Morari, 1988a). This value should be less than one at all frequencies for the system to have RS.

Nominal performance (NP)—To test for NP we simply compute $\bar{\sigma}(\omega_P S)$ as a function of frequency. It should be less than one at all frequencies (or equivalently $\|w_P S\|_\infty < 1$) for NP to be satisfied.

Robust performance (RP)—This is satisfied if the above-mentioned performance criterion is satisfied for all possible model errors. Mathematically, this is tested by computing μ of the matrix N_{RP} (see Skogestad and Morari, 1988a):

$$N_{RP} = \begin{pmatrix} w_I CSG & w_I CS \\ w_P SG & w_P S \end{pmatrix}, \qquad (12)$$

$\mu(N_{RP})$ should be less than one at all frequencies for RP to be satisfied. The peak value of $\mu(N_{RP})$ will be denoted μ_{RP}. Note that satisfying NP and RS is a prerequisite for satisfying RP.

2.4. Modelling

The objective of this paper is to evaluate the achievable robust performance of distillation columns using the LV-configuration. As example columns we will use the seven columns A–G used by Skogestad and Morari (1988b). Steady-state data for those columns are summarized in Table 1. These

Table 1. Steady-state data for distillation column examples. All columns have liquid feed ($q_F = 1$)

Column	z_F	α	N	N_F	$1 - y_D$	x_B	D/F	L/F	λ_{11}
A	0.5	1.5	40	21	0.01	0.01	0.500	2.706	35.1
B	0.1	1.5	40	21	0.01	0.01	0.092	2.329	47.5
C	0.5	1.5	40	21	0.10	0.002	0.555	2.737	7.53
D	0.65	1.12	110	39	0.005	0.10	0.614	11.862	58.7
E	0.2	5	15	5	0.0001	0.05	0.158	0.226	2.82
F	0.5	15	10	5	0.0001	0.0001	0.500	0.227	499
G	0.5	1.5	80	40	0.0001	0.0001	0.500	2.635	1673

columns are chosen to represent a reasonable sample of high-purity distillation towers which from the literature (e.g. Shinskey, 1984) one might expect are difficult to control using the LV-configuration. The steady-state RGA-values are also shown in Table 1. They are in the range from 3 to 1700 for the seven columns.

The results in this paper are based on the following assumptions: binary distillation, constant molar flows, constant relative volatility, negligible vapour holdup and vapour–liquid equilibrium as well as perfect mixing on all stages. Note that the liquid flow dynamics are not neglected, and a simple linear relationship is used: $\Delta L_i(t) = \Delta M_i(t)/\tau_L$. This gives for each tray two ordinary differential equations, one for composition and one for liquid holdup. All stages, including reboiler and condenser, are assumed to have identical holdups $M_i/F = 0.5$ min, $\tau_L = \theta_L/(N-1)$ is assumed equal for all trays. The value of the overall liquid lag θ_L is given in Table 2. We also assume perfect control of levels and pressure, i.e. constant M_D, M_B and p. This assumption is justified by considering the fast dynamic response of levels and pressure compared to the response of compositions. Furthermore, the behavior of the LV-configuration is insensitive to the level control.

A linear model, which is denoted the "full" linear model in the following, is obtained by linearizing the nonlinear model around the nominal steady-state. In addition, the following simplified linear model (two-time constant model with flow dynamics) is used (Skogestad and Morari, 1988b):

Table 2. Data used in simple model of distillation columns, equation (13)

Column	$G_{LV}(0)^a$	τ_1	τ_2	θ_L
A	$\begin{pmatrix} 87.8 & -86.4 \\ 108.2 & -109.6 \end{pmatrix}$	194	15	2.46
B	$\begin{pmatrix} 174.79 & -171.7 \\ 90.191 & -90.5 \end{pmatrix}$	250	15	2.86
C	$\begin{pmatrix} 16.023 & -16.0 \\ 9.29 & -10.7 \end{pmatrix}$	24	10	2.44
D	$\begin{pmatrix} 24.585 & -24.2 \\ 21.270 & -21.3 \end{pmatrix}$	154	30	1.54
E	$\begin{pmatrix} 203.4 & -131.5 \\ 22.47 & -22.5 \end{pmatrix}$	82	30	11.06
F	$\begin{pmatrix} 10{,}740 & -10{,}730 \\ 9257 & -9267 \end{pmatrix}$	2996	4	7.34
G	$\begin{pmatrix} 8648.94 & -8646 \\ 11{,}347.06 & -11{,}350 \end{pmatrix}$	20,333	30	5.06

$$dy_D = \frac{k_{11}}{1+\tau_1 s}\,dL + \left(\frac{k_{11}+k_{12}}{1+\tau_2 s} - \frac{k_{11}}{1+\tau_2 s}\right) dV,$$

$$dx_B = \frac{k_{21}}{1+\tau_1 s} g_L(s)\,dL + \left(\frac{k_{21}+k_{22}}{1+\tau_2 s} - \frac{k_{21}}{1+\tau_1 s}\right) dV. \tag{13}$$

This simple model includes the liquid flow dynamics and the differences between changes in external and internal flows. k_{ij} denotes the steady-state gain around the normal operating point. These values are easily obtained from steady-state simulations, but were obtained here by linearizing the model. τ_1 and τ_2 are the time constants associated with changes in external flows and internal flows, respectively. $g_L(s)$ expresses the liquid flow dynamics:

$$g_L(s) = \frac{1}{[1 + (\theta_L/n)s]^n}, \tag{14}$$

where θ_L is the overall liquid lag from the top to the bottom of the column. n in equation (14) should be equal to the number of trays $N - 1$ in the column, but is throughout this paper chosen to be five to avoid a model of unnecessary high order. Data for the simple model (13) are given in Table 2 for the seven example columns. Note that all gains used in this paper are for scaled (logarithmic) compositions:

$$y_D^S = \frac{y_D}{1 - y_D^\circ}, \quad x_B^S = \frac{x_B}{x_B^\circ}. \tag{15}$$

Here x_B° and $1\text{-}y_D^\circ$ are the amounts of impurity in each product at the nominal operating point. The use of logarithmic compositions scales the outputs in a comparable manner for performance, and in addition linearizes the plant.

To study the effect of modelling accuracy on the results we shall design controllers for four special cases of equation (13) in addition to the full linear model:

- **N1:** $\tau_2 = \tau_1$, $\theta_L = 0$. Simplest model with only the dominating time constant τ_1 and neglected flow dynamics.
- **N2:** $\theta_L = 0$. Two-time constant model with neglected flow dynamics.
- **F1:** $\tau_2 = \tau_1$. One time-constant model with θ_L as in Table 2.
- **F2:** Two time-constant model with τ_1, τ_2 and θ_L as in Table 2.
- **Full:** Model obtained by linearizing the full nonlinear model.

Here N is used to indicate "no flow dynamics", F means "flow dynamics", and 1 and 2 means that the model uses one or two time constants, respectively.

2.5. Controllers

We use two different approaches to tune the controllers.

Approach 1—In the first approach we fix the performance specification and minimize μ_{RP} [the peak value of $\mu(N_{RP})$] by adjusting the controller tunings. The performance requirement is satisfied if μ_{RP} is less than one, and lower μ_{RP}-values represent a better design. Physically, a μ_{RP}-value of say 0.7 means that both the uncertainty weight and performance weight may be increased by a factor of 1/0.7 at all frequencies and still have robust performance with the new problem definition. Approach 1 with the simple performance weight w_{P1} [equation (9)] is used in the majority of the cases in this paper.

Approach 2—A more meaningful approach is probably to fix the uncertainty and find what performance can be achieved for this plant. In the second approach we therefore adjust the time constant τ_P in the performance weight (or equivalently adjust the bandwidth ω_B of the weight) to make the optimal μ_{RP}-value equal to one. The optimization problem is then:

$$\min_{\tau_P} |[\min_{C} \mu_{RP}(C, \tau_P)] - 1|. \tag{16}$$

Different designs may then be compared based on their maximum achievable bandwidth. Two disadvantages with this approach are: (1) it introduces an outer loop in the μ-calculations; (2) it may be impossible to achieve μ_{RP} equal to one by adjusting τ_P in the performance weight. This may be the case if the high-frequency specification (value of M in the weight) is limiting. A more difficult case arises when the system is not even robustly stable ($\mu_{RS} > 1$), and even adjusting M would not help.

μ-optimal controller—The term "μ-optimal controller" is used to denote a linear multivariable controller with an "unlimited" number of states obtained by minimizing the peak of $\mu(N_{RP})$, that is, a controller designed to give the best possible performance for the worst combination of uncertainty, disturbances etc.

PID controllers—"Optimal PID-settings" denote the parameter settings for single-loop PID-controllers found either by minimizing μ_{RP} according to Approach 1, or by minimizing the performance weight time constant τ_P according to Approach 2. These settings are found by a general optimization routine and since there are many local minima there is no guarantee that the settings presented in this paper really are the true optimal. However, since a large number of optimizations have been performed we believe it is unlikely to find setting with significantly lower μ_{RP}-values (or τ_P-values), than those presented here.

The PID-controllers considered in this paper are on the cascade form with the derivative action assumed to be effective over one decade:

$$C_{PID}(s) = k \frac{1 + \tau_1 s}{\tau_1 s} \frac{1 + \tau_D s}{1 + 0.1\tau_D s}. \tag{17}$$

It is assumed that reflux L is used to control top compositions y_D and boilup V is used to control bottom composition x_B. Subscripts x and y on the tuning parameters are used to denote the respective loops. The gains k_y and k_x are for scaled compositions as described by equation (15).

2.6. Simulations

The robust performance analysis using μ is the main basis for comparison and simulations are only intended to illustrate these results. All simulations are for column A using the full non-linear model with flow dynamics. Since all simulations using single-loop controllers which generally are insensitive to steady-state input errors (Skogestad and Morari, 1987), no steady-state input error is included in the simulations (although 20% is allowed for in the uncertainty description). However, to penalize fast controller actions all simulations do include a "time delay" θ in each channel [actually, it is a fifth-order lag $1/(1 + \theta s/5)^5$] as allowed for by the uncertainty description. $\theta = 1$ min unless specified otherwise. All simulations with step changes in setpoints include the prefilter c_f [equation (11)] which has a time constant of 5 min.

3. RESULTS

3.1. Results for Column A

RGA-analysis of models—In Fig. 8 we plot the magnitude of the diagonal elements of the RGA as a function of frequency for the five different models of Column A (note that $\lambda_{11} = \lambda_{22}$ for 2×2 plants). The true plant (as given by the full model) has large RGA-values at steady state, but at high frequencies λ_{11} is equal to one. The simple model N1 gives a constant value of $\lambda_{11} = 35$ at all frequencies. Including

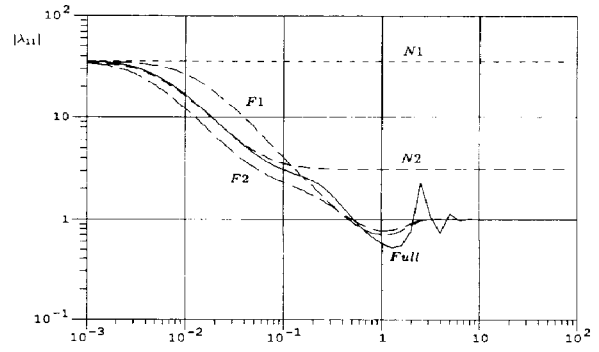

Fig. 8. $|\lambda_{11}|$ vs frequency for all process models of Column A.

Table 3. μ_{RP}-optimal PID tunings for different models of Column A (weight w_{P1}, $\tau_{P1} = 10$ min, Approach 1)

Model	μ_{RP}	k_y	k_x	τ_{Iy} (min)	τ_{Ix} (min)	τ_{Dy} (min)	τ_{Dx} (min)
N1	1.32	4.38	1.30	179	1.87	0.32	0.23
N2	0.84	0.65	0.45	12.2	4.31	0.51	0.47
F1	0.91	0.85	0.38	7.77	3.61	0.81	1.11
F2	0.80	0.38	0.36	6.49	5.80	1.13	0.91
Full	0.86	0.22	0.32	3.51	4.71	1.22	0.61

the flow dynamics (F1) gives RGA-values similar to the true ones, and including also τ_2 (F2) improves the model somewhat at intermediate frequencies.

PID tunings for all models—Optimal PID-tunings and the corresponding μ_{RP} values are shown in Table 3 for all five models of Column A. Note that μ_{RP} decreases when flow dynamics and/or τ_2 are included in the model. The reason for this is that both these effects make the process less ill-conditioned (smaller RGA-values), and thereby less sensitive to the uncertainty on the inputs and therefore simpler to control (Skogestad and Morari, 1987). Figure 9 displays $\mu(N_{RP})$ for the controller settings of Table 3 when applied to the *full* linear model, and the corresponding μ_{RP} values are summarized in Table 4. These results tell how well-suited the simplified models are for designing controllers for the actual plant. As expected, model N1 gives a controller with poor performance when applied to the full model, while model F2 yields a controller which performs well; the controller based on F2 yields a μ_{RP}-value of 0.95 which is reasonably close to the optimal value of 0.86 obtained by designing the controller for the full model. Simulations of a setpoint change in y_D using the controllers based on: (i) the simple model F2; and (ii) the full model are shown in Fig. 10. The results confirm that model F2 is adequate for controller design for Column A.

Comparison with μ-*optimal controller*—Skogestad and Morari (1988a) report the "μ-optimal" controller (multivariable) for model N2 to give $\mu_{RP} = 0.955$. As shown in Table 3 it is possible to achieve μ_{RP} equal to 0.843 using two single-loop PID-controllers. The reason for these contradicting

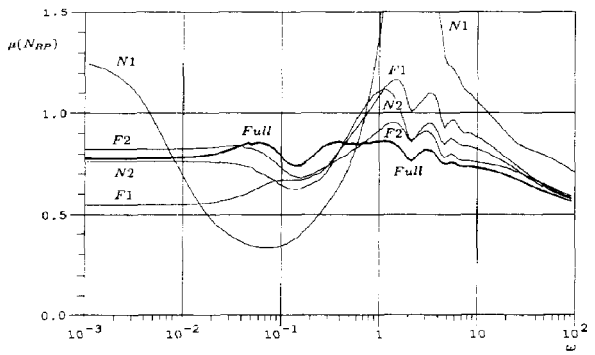

Fig. 9. $\mu(N_{RP})$-plots for different PID controllers (Table 3) applied to the full linear model of Column A.

results is simply that the software package used by Skogestad and Morari was still at the development stage and did not yield the true optimum.

One might wonder if there is any benefit in introducing multivariable effects in the controller for Column A. To test this we optimized the parameters in a multivariable controller $C(s) = C(sI - A)^{-1}B + D$ with four states (including two fixed integrators). This controller has 18 adjustable parameters (using a canonical form as shown in Fig. 11). Note that this controller is not equal to a conventional "multivariable PID-controller" which would have six states and 12 parameters (or 16 parameters if the range of the derivative action is not fixed). We were able to reduce μ_{RP} from 0.843 (two single-loop PIDs) to 0.832 (general four-states controller) for model N2, and from 0.799 to 0.766 for model F2. These results indicate that the performance achieved by using two single-loop controllers is close to the optimal for Column A.

Comparison of PI- and PID-controllers—Table 5 shows the PI- and PID-tunings and corresponding μ_{RP}-values for model F2. We see from these results that there is a significant improvement by introducing the derivative action. In fact this is true for all the studied columns except Column E, which is only marginally improved.

Choice of performance weight and optimization approach—To study this effect we obtained PID tunings for model F2 using both weights w_{P1} and w_{P2} and using both Approaches 1 and 2. The result for the four cases are shown in Table 6. When Approach 1 is used we see that the different weights result in somewhat different tunings; the main difference is that weight w_{P2} gives higher controller gains than w_{P1}. This is not surprising since weight w_{P2} requires more performance than w_{P1} (see Fig. 7). If we use Approach 2 (τ_P in the weight is minimized such that the optimal μ_{RP} is one) then the difference between the two weights is only minor. This is seen from the last two rows of Table 6. The values of the minimized time

Table 4. μ_{RP}-values for controller settings of Table 3 when applied to the *full* linear model of Column A

Controller (Table 3)	μ_{RP} Original	μ_{RP} Full model
N1	1.32	2.53
N2	0.84	1.11
F1	0.91	1.17
F2	0.80	0.95
Full	0.86	0.86

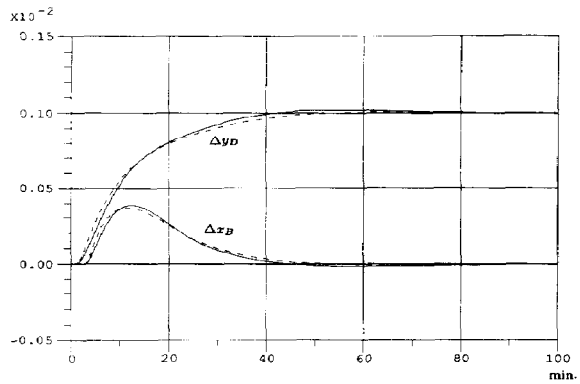

Fig. 10. Goodness of model F2 for controller tuning. Closed-loop simulation of setpoint-change in y_D for PID-controllers (Table 3) based on the full linear model (——) and based on model F2 (- - -).

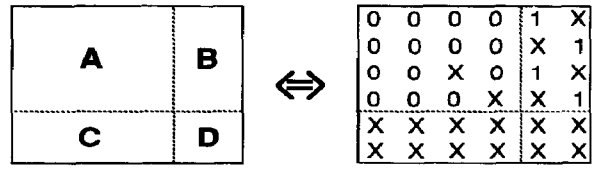

Fig. 11. Canonical form of multivariable controller $C(s) = C(sI - A)^{-1}B + D$ with four states (including two fixed integrators). Zeros and ones are constants, Xs are adjustable parameters.

constant in the weights are, of course, different ($\tau_{P1} = 3$ min and $\tau_{P2} = 10$ min), but the optimal PID tunings are similar. This is confirmed by simulations in Fig. 12 which show the response to a simultaneous step disturbance in feed composition and feed flow using these two controllers. Figure 12 also shows that good disturbance rejection may be obtained using the weighted sensitivity function $w_P S$ as a performance measure.

Effect of detuning controllers—The RGA-plot shows that interactions are most severe at low frequency, and that they may almost disappear if it is possible to have the closed-loop bandwidth sufficiently high. This suggests that if a well-tuned controller (high bandwidth) is detuned then interaction will become more severe. This is indeed confirmed by the simulations in Fig. 13 where the controller gain k for both loops has been reduced by the same factor. The intuitive reaction for an operator who encounters large interactions is probably to detune the controllers. In this case this is seen to yield exactly the opposite effect of what is expected.

Effect of measurements delays (uncertainty weight)—The RGA-plots also suggest that large measurements delays may be detrimental for the LV-configuration, because a large delay forces one to operate with a low closed-loop bandwidth and one gets into the region where the interactions are large which makes performance even worse. This is confirmed by increasing the allowed time delay θ in the uncertainty weight [equation (1)] from 1 to 6 min, and computing the achievable closed-loop time constant τ_{P1} according to Approach 2. The results are summarized in Table 7. We must see that increasing the time delay from 1 to 6 min implies that τ_{P1} must be increased from 3 to 55 min, that is, achievable performance is expected to be seriously affected if, for example, measurement delays are present. The simulation results in Fig. 14 which show disturbance responses for the two controllers tuned for a 1 and 6 min time delay, respectively, clearly demonstrate that this is the case.

One-point control and decentralized tuning—PID tunings for one-point control (when only one output matters in the H_∞ objective function) were obtained with Approach 2 with weight w_{P2} and the results summarized in Table 8. The results show that it is possible to achieve very tight control of the individual loops; we find for both single loops $\tau_{P2} < 1.8$ min. We note that the μ-optimal integral time is 3–4 times longer than would be obtained using Ziegler–Nichols tuning rules, but the gain and derivative time are quite similar [for a process $100\,e^{-\theta s}/(1 + 194s)$ which includes a time delay θ (= 1 min), the Zieger–Nichols tuning rules yield approx. $k = 1.8/\theta$(= 1.8), $\tau_I = 2\theta$ (= 2 min), and $\tau_D = \theta/2$ (= 0.5 min)].

The most interesting question is if these "one-point" tunings may be used for two-point control. Recall that for two-point control the best achievable performance (Approach 2 with both loops optimized simultaneously) corresponds to $\tau_{P2} = 10$ min (last entry in Table 6). We note that these "two-point" tunings have both k and τ_I about half of those obtained for "one-point" tuning (Table 8). When we hold $\tau_{P2} = 10$ min fixed (Approach 1), and evaluate how the "one-point" tunings perform when both loops are closed simultaneously, we obtain $\mu_{RP} = 1.18$, which is only 18% higher than the optimal "two-point" tunings. This is somewhat surprising since the large RGA-values (35.1 at steady-state, see Table 1) are supposed to indicate large changes in the gains as we open or close loops (Bristol, 1966). The reason why the difference is small is again that the closed-loop bandwidth is sufficiently large, such that RGA-values in the frequency range of importance are close to one. However, the closed-loop system based

Table 5. μ_{RP}-optimal PI- and PID-tunings for model F2, Column A (weight w_{P1}, Approach 1)

Controller	μ_{RP}	k_y	k_x	τ_{Iy} (min)	τ_{Ix} (min)	τ_{Dy} (min)	τ_{Dx} (min)
PI	0.94	0.14	0.62	2.74	13.1		
PID	0.80	0.38	0.36	6.49	5.80	1.13	0.91

Table 6. μ_{RP}-optimal PID-tunings for Column A, model F2. Effect of performance weight (w_{P1}, w_{P2}) and tuning approach

Approach	Weight	τ_P (min)	μ_{RP}	k_y	k_x	τ_{Iy} (min)	τ_{Ix} (min)	τ_{Dy} (min)	τ_{Dx} (min)
1	w_{P1}	10	0.80	0.38	0.36	6.49	5.80	1.13	0.91
1	w_{P2}	16.7	0.91	0.74	0.55	6.09	4.46	1.06	0.74
2	w_{P1}	3	1	0.67	0.72	3.58	4.34	1.34	0.76
2	w_{P2}	10	1	0.86	0.69	4.61	3.76	1.22	0.59

on "one-point" tunings is close to instability ($\mu_{RS} > 0.8$), and the "one-point" gains should be detuned somewhat to achieve acceptable robustness.

3.2. Results for all columns

Robust performance with LV-configuration—The optimal PID-settings for all Columns A–G are shown in Tables 9 and 10 for models N2 (no flow dynamics) and F2 (flow dynamics) respectively. Except for one case, all μ_{RP}-values are less than one. These results show that robust performance is indeed possible with the LV-configuration for a wide range of columns when the measurement delays are limited to about 1 min.

Relationship to RGA—Note especially Columns F and G which have good performance even though they have extremely high RGA values at steady-state. This shows that there is no direct relation between the RGA-value at steady-state and achievable control performance. However, if we consider the RGA in the *crossover* region (frequency about 0.1 min^{-1}) there is a much better correlation. For model N2 the RGA at high frequency is approximately equal to L/F (Skogestad and Morari, 1988b) which correlates well with the μ_{RP}-values in Table 9. For model F2 the RGA at high frequency is low for columns with large θ_L; again this correlates well with the μ_{RP}-values in Table 10.

Effect of flow dynamics on performance—Including flow dynamics gives a more complicated model and also introduces an effective dead time from the top to the bottom of the column. Still, we find that including flow dynamics makes PID-control simpler for Columns A, D and G. This may also be explained in terms of the lower RGA-values when flow dynamics are included. The largest improvement is found for Column D which also has the largest reduction in RGA-values.

Tuning rules—It is not possible directly from Tables 9 and 10 to derive any simple tuning rules in terms of the time constants of the process given in Table 2. Though some conclusions can be made. There is definitely no relationship to the dominant time constant τ_1. It is also difficult from our data to find any correlation with θ_L. There seems to be some correlation between the integral time τ_I and τ_2. A more careful analysis based on loop shaping arguments (e.g. Doyle and Stein, 1981) shows that at low to intermediate frequencies the controller should try to give large gains in the low-gain direction, $\sigma_{min}(G)$. For the simple model N2 this direction has a pole at $1/\tau_2$ and it is optimal to choose the integral time τ_I approximately at this location to counteract for its effect. A good rule seems to be $\tau_I \approx \tau_2/2$ provided $\tau_I > 3\theta$, where θ is the dead time. For the full column model (and model F2) the situation is more complicated. There is still a pole close to $1/\tau_2$, but also poles and zeros at higher frequencies and their positions affect the optimal tuning of τ_I. However, comparing Table 9 with Table 10 shows that including the flow dynamics generally has the effect that τ_I can be decreased and thereby improving the performance.

For the derivative time it is a common rule of thumb to choose $\tau_D = \theta/2$ (e.g. Ziegler–Nichols for first-order process with dead-time θ). This value is indeed close to what was obtained by optimizing the

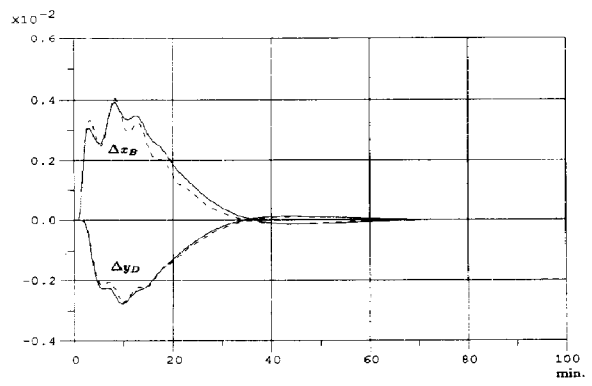

Fig. 12. Effect of different performance weights with Approach 2. Closed-loop simulation of simultaneous disturbances in F (+30%) and z_F (+20%). PID-controllers tuned using w_{P1} (solid line) and w_{P2} (dotted line).

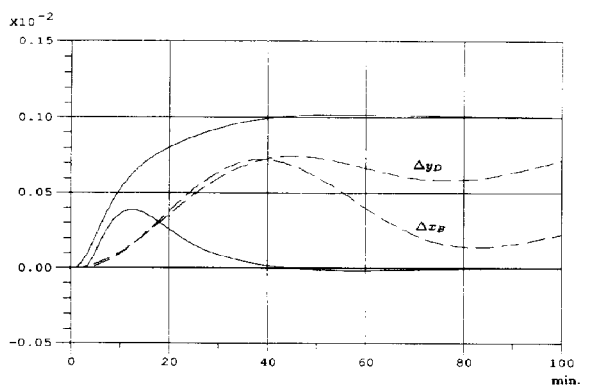

Fig. 13. Effect of detuning. Closed-loop simulation of set-point-change in y_D using PID-tunings from entry "full" in Table 3. Solid lines = original settings; dotted lines = gains reduced by a factor of 10.

Table 7. μ_{RP}-optimal PID-tunings for Column A, model F2, for different values of θ in the uncertainty weight (weight w_{P1}, Approach 2)

θ (min)	τ_{P1} (min)	μ_{RP}	k_y	k_x	τ_{Iy} (min)	τ_{Ix} (min)	τ_{Dy} (min)	τ_{Dx} (min)
1	3	1	0.67	0.72	3.58	4.34	1.34	0.76
6	55	1	0.14	0.12	16.6	14.3	3.17	3.54

PID parameters with respect to robust performance (see Tables 8–10).

4. DISCUSSION

The control performances of the controllers and columns was compared based on robust performance using the structured singular value μ. This provides a simple and rigorous means for comparison which does not depend on a number of arbitrary choices as is the case for the traditional simulation approach. We have also used simulations to illustrate the validity of the μ-analysis, and the correction has generally been good. However, one should note that the simulations shown are for specific choices of setpoint changes, disturbances and model error. One should not necessarily expect a correlation between a single simulation and the worst-case response (worst-case combination of setpoints, disturbances and model errors) for which μ is a measure. One of the main advantages with the μ-analysis as opposed to simulations is that one does not have to search for the worst case—μ finds it automatically.

We would like to stress that the problem formulation used in this paper using weighted sensitivity ($\|w_P S\|_\infty$) for performance and only input uncertainty, was derived by looking for something simple which is also physically meaningful. In general, one may for performance also include noise on the measurements, include disturbances and setpoints directly, and penalize the magnitude of the input signals. Furthermore, other sources of uncertainty could be included. These additional specifications may easily be included in the μ-analysis. However,

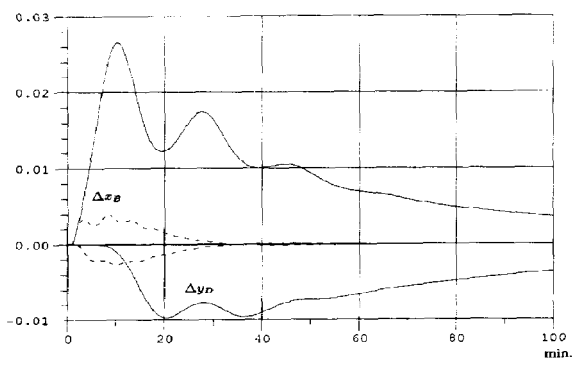

Fig. 14. Effect of increased measurement delay θ. Closed-loop simulation of simultaneous disturbances in F (+30%) and z_F (+20%). Solid line: $\theta = 6$ min; dotted line: $\theta = 1$ min. Optimal PID-tunings for the two cases from Table 7.

for the present problem we believe that the most important aspects are captured by the very simple problem definition used here. The reasons are: (1) that the input uncertainty seems to be the most severe uncertainty for this system; and (2) that most performance specifications may be captured using weighted sensitivity.

In the paper we have represented time delays as input uncertainty using equation (1). In most cases this time delay is caused by delayed composition measurements. Two things might be questioned: (1) is it reasonable to model time delays as model uncertainty? and (2) is it reasonable to model measurement delays which occur at the *ouput* as *input* uncertainty? The answer to the first question is "yes", and the reason is that the time delay in almost all cases will be the "worse-case" error which can be modelled by the uncertainty bound. The answer to the second question is in general "no" because uncertainty at the inputs usually limits performance more than does uncertainty at the outputs (e.g. Skogestad *et al.*, 1988). However, since we in this paper analyze only single-loop controllers (C is diagonal) it is acceptable because the uncertainty in each loop may be "shifted" through the controllers without adding conservativeness.

One major difficulty in obtaining PID tuning rules for the example columns is that there is a large number of parameter values which yield about the same μ-value. This of course also makes the parameter optimization very difficult. In particular, we observed that making one loop faster and the other slower generally only had a small effect on the optimal value of μ. In fact, for some of the columns with large interactions, e.g. model N1, the best choice is to make one loop fast and the other slow, and one gets about the same optimal μ-value irrespectively of what loops one selects as the fast one. These issues, which also imply that the optimal solution is nonunique for certain problems, is discussed in more detail by Skogestad *et al.* (1989).

In the paper we found that the LV-configuration may yield acceptable performance provided measurement delays are not too large (less than 1–2 min); for the columns studied it is possible to obtain closed-loop time constants less than 10 min in spite of the fact that the dominating open-loop time constant (τ_1) may be hundreds of minutes. This does not imply that the LV-configuration is the best structure to use—others may even be better. For example, the $(L/D)(V/B)$-configuration is probably better in most cases, and in particular for columns with large reflux. We also found that for the LV-configuration a

Table 8. μ_{RP}-optimal one-point PID-tunings for Column A, model F2 (weight w_{P2}, Approach 2)

Closed-loop	τ_P (min)	μ_{RP}	k_y	k_x	τ_{Iy} (min)	τ_{Ix} (min)	τ_{Dy} (min)	τ_{Dx} (min)
Top	1.75	1	2.07		6.42		0.49	
Bottom	1.80	1		1.46		8.46		0.48

Table 9. μ_{RP}-optimal PID-tunings for model N2 (weight w_{P1}, Approach 1)

Column	μ_{RP}	k_y	k_x	τ_{Iy} (min)	τ_{Ix} (min)	τ_{Dy} (min)	τ_{Dx} (min)
A	0.84	0.65	0.45	12.2	4.31	0.51	0.47
B	0.84	0.41	0.66	3.16	10.7	0.71	0.36
C	0.86	0.60	0.48	4.88	4.93	0.48	0.42
D	1.13	5.76	5.78	15.0	15.0	0.32	0.32
E	0.74	0.13	0.88	15.1	15.2	0.50	0.47
F	0.77	0.043	0.059	5.92	4.66	0.81	0.49
G	0.87	0.69	0.61	22.0	12.4	0.41	0.36

Table 10. μ_{RP}-optimal PID-tunings for model F2 (weight w_{P1}, Approach 1)

Column	μ_{RP}	k_y	k_x	τ_{Iy} (min)	τ_{Ix} (min)	τ_{Dy} (min)	τ_{Dx} (min)
A	0.80	0.38	0.36	6.49	5.80	1.13	0.91
B	0.85	0.51	0.36	9.33	4.21	0.79	0.72
C	0.87	0.32	0.40	2.99	5.22	1.00	1.02
D	0.91	2.65	1.02	7.45	2.78	0.87	0.20
E	0.75	0.15	0.66	17.8	21.1	0.50	0.43
F	0.81	0.044	0.093	6.06	8.96	1.82	0.39
G	0.77	0.35	0.37	11.9	11.8	1.31	0.79

well-tuned PI- or PID-controller may be close to the best you can do. Again, we stress that this conclusion does not necessarily apply to other configurations. For example, for the DV-configuration, multivariable controllers which include decoupling effects may be much better than using single-loop PID-controllers.

It is obvious from our results that time delays impose serious limitations on performance when using the LV-configuration. To obtain good control quality with this configuration it is therefore critical to minimize delays due to composition measurements, for example, by estimating (inferring) compositions from temperature measurements.

5. CONCLUSION

We shall summarize our conclusions with regards to two-point distillation control using the LV-configuration by briefly answering the seven questions raised in the Introduction.

1. It is possible to achieve good control behavior using the LV-configuration for two-point composition control provided measurements delays are not too large (typically less than 1–2 min).
2. The severe interactions and poor control often reported with the LV-configuration may be almost eliminated if the loops are tuned sufficiently tight. Again, this is possible only if the measurement delays are relatively small (less than 1–2 min).
3. Because of model uncertainty single-loop control using PID-controllers seems close to the best multivariable controller for the LV-configuration.
4. The most important model characteristic for controller tuning is the high-frequency dynamics (initial response). For example, it is critical to include flow dynamics (θ_L) and measurement delays (θ). The dominating dynamics (steady-state gains and dominant time constant τ_1) are much less important for controller design. Including the effect of changes in internal flows (τ_2) improves the controller design somewhat.
5. There is no correlation between the steady-state RGA-value and the achievable control performance. On the other hand, the RGA-values at high frequency correlate quite well.
6. Provided the loops can be tuned sufficiently tight, the same controller tunings may work satisfactory, both for one-point and two-point control.
7. The optimal PID-tunings are not at all related to the slow dynamics as represented by the dominating time constant τ_1. The integral time is generally smaller and choosing it as $\tau_2/2$ is reasonable in many cases provided this value is at least three times the dead time. The derivative time may be chosen as approximatley half of the effective dead time in each loop.

The structured singular value (μ) was used as a tool for evaluating the achievable control performance. Performance was defined in terms of the H_∞-norm of the weighted sensitivity function $w_P S$, and the issue of selecting an appropriate weight w_P was discussed in detail. It was shown:

1. Most performance specifications, including disturbance rejection, may be handled using a simple scalar weight w_P.

2. In this particular example with the LV-configuration and PID-controllers the exact *shape* of the weight (w_{P1} or w_{P2}) is not critical. This implies, for example, that the results do not depend on whether the disturbances (or set-points) appear at the outputs as steps or ramps.
3. However, the results (in terms of optimal PID tunings) do depend on the choice of the parameters in the weight w_P. The last sensitivity may be avoided by adjusting the parameters in w_P such that the best achievable performance for a given uncertainty is obtained ("Approach 2").

NOMENCLATURE†

$C(s)$ = Controller
$G(s)$ = Linear model of column
k_{ij} = Steady state gains for column
RGA = Relative gain array, elements are λ_{ij}
$S(s) = [I + G(s)C(s)]^{-1}$, sensitivity function
w_I = Uncertainty weight
w_P = Peformance weight
x_B = Mol fraction of light component in bottom product
y_D = Mol fraction of light component in distillate (top product)

Greek symbols

$\|A\|_\infty = \max_\omega \bar{\sigma}[A(j\omega)] = H_\infty$-norm of matrix A
$\lambda_{11}(j\omega) = [1 - g_{12}(j\omega)g_{21}(j\omega)/g_{11}(j\omega)g_{22}(j\omega)]^{-1} = 1,1$ element in RGA.
ω = frequency (min^{-1})
$\bar{\sigma}, \sigma_{min}$ = Maximum and minimum singular values
μ = Structured singular value
$\mu_{RP} = \max_\omega \mu(N_{RP})$ = peak value of μ for robust performance
τ_1 = Dominant time constant for external flows (min)
τ_2 = Time constant for internal flows (min)
θ = Measurement delay (min)
θ_L = Overall lag for liquid response (min)

†See also Figs 1 and 3.

REFERENCES

Arkun Y. and C. O. Morgan III, On the use of the structured singular value for robustness analysis of distillation column control. *Comput. chem. Engng* **12,** 303–306 (1988).

Bristol E. H., On a new measure of interactions for multivariable process control. *IEEE Trans. Automat. Control.* **AC-11,** 133–134 (1966).

Doyle J. C., Analysis of feedback systems with structured uncertainties. *IEEE Proc.* **129,** 242–250 (1982).

Doyle J. C. and G. Stein, Multivariable feedback design: concepts for a classical/modern synthesis. *IEEE Trans. Automat. Control.* **AC-26,** 4–16 (1981).

McDonald K. A., A. Palazoglu and B. W. Bequette, Impact of model uncertainty descriptions for high-purity distillation control. *AIChE Jl* **34,** 1996–2004 (1988).

Nett C. N., Presentation at the *1987 Am. Control. Conf.*, Minneapolis (1987).

Shinskey F. G., *Distillation Control*, 2nd Edn. McGraw-Hill, New York (1984.)

Skogestad S. and M. Morari, Implication of large RGA-elements on control performance. *Ind. Engng Chem. Res.* **26,** 2121–2330 (1987).

Skogestad S. and M. Morari, LV-control of a high-purity distillation column. *Chem. Engng Sci.* **43,** 33–48 (1988a).

Skogestad S. and M. Morari, Understanding the dynamic behavior of distillation columns. *Ind. Engng Chem. Res.* **27,** 1848–1862 (1988b).

Skogestad S., M. Morari and J. C. Doyle, Robust control of ill-conditioned plants: high-purity distillation. *IEEE Automat. Control* **33,** 1092–1105 (1988).

Skogestad S., P. Lundström and M. Hovd, Control of identical parallel processes. Presented at *AIChE Annual Meeting*, San Francisco (1989).